Understeer characteristics for energy-efficient fully electric vehicles with multiple motors

LENZO, Basilio <http://orcid.org/0000-0002-8520-7953>, SORNIOTTI, A, DE FILIPPIS, G, GRUBER, P and SANNEN, K

Published version

LENZO, Basilio, SORNIOTTI, A, DE FILIPPIS, G, GRUBER, P and SANNEN, K (2016). Understeer characteristics for energy-efficient fully electric vehicles with multiple motors. In: EVS29 International Battery, Hybrid and Fuel Cell Electric Vehicle Symposium Proceedings, Montreal, Quebec, 19-22 June 2016. (Unpublished)

Copyright and re-use policy

EVS29 Symposium
Montréal, Québec, Canada, June 19-22, 2016

Understeer characteristics for energy-efficient fully electric vehicles with multiple motors

Basilio Lenzo[1], Giovanni De Filippis[1], Aldo Sorniotti[1], Patrick Gruber[1], Koen Sannen[2]

[1]*University of Surrey, Guildford, Surrey, GU2 7XH, UK.* a.sorniotti@surrey.ac.uk

[2]*Flanders MAKE, 3920 Lommel, Belgium*

Summary

Electric vehicles with multiple motors allow torque-vectoring, which generates a yaw moment by assigning different motor torques at the left and right wheels. This permits designing the steady-state cornering response according to several vehicle handling quality targets. For example, as widely discussed in the literature, to make the vehicle more sports-oriented, it is possible to reduce the understeer gradient and increase the maximum lateral acceleration with respect to the same vehicle without torque-vectoring. This paper focuses on the novel experimentally-based design of a reference vehicle understeer characteristic providing energy efficiency enhancement over the whole range of achievable lateral accelerations. Experiments show that an appropriate tuning of the reference understeer characteristic, i.e., the reference yaw rate of the torque-vectoring controller, can bring energy savings of up to ~11% for a case study four-wheel-drive electric vehicle demonstrator. Moreover, during constant speed cornering, it is more efficient to significantly reduce the level of vehicle understeer, with respect to the same vehicle with even torque distribution on the left and right wheels.

Keywords: torque-vectoring, cornering, energy consumption, understeer characteristic

1 Introduction

Electric vehicles (EVs) with multiple motors allow the design of the cornering response through torque-vectoring strategies that generate a yaw moment, caused by the different electric motor torques at the left and right wheels [1-3]. Hence, the same vehicle hardware can originate different understeer characteristics (i.e., the graphs of steering wheel angle as a function of lateral acceleration for steady-state conditions), depending on the tuning of the torque-vectoring controller.

According to the literature, the design of the reference understeer characteristic for a vehicle with torque-vectoring capability can aim at: i) reducing the understeer gradient with respect to the passive vehicle (i.e., the same vehicle plant without the torque-vectoring controller); ii) extending the region of linear cornering response; and iii) extending the range of possible lateral accelerations for the available tire-road friction conditions [4]. Objectives i)-iii) allow achieving a more sports-oriented vehicle behavior. On the other hand, because of the influence of direct yaw moment control on drivetrain power losses and tire slip power losses, the reference understeer characteristic has an impact on energy efficiency [5].

Drivetrain power losses and tire slip power losses are major sources of power consumption in vehicles. In EVs, drivetrain power losses include the contributions of the inverters, electric motors and transmissions (if present, e.g., in the case of on-board electric drivetrains). In general, these losses are functions of the torque

and speed conditions of each drivetrain. The dissipation due to longitudinal and lateral tire slips becomes relevant only at significant longitudinal and/or lateral accelerations. For a vehicle without torque-vectoring the longitudinal slips are different between the inner and outer driven wheels during cornering, because of the lateral load transfers. The increased vertical load on the outer tires implies that smaller slip ratios are needed to generate the same traction force as on the inner tires. Torque-vectoring allows conveniently distributing the traction forces among the left and right wheels. More specifically, a reduction of vehicle understeer in traction (see objective i)) is achieved by increasing the longitudinal forces on the outer wheels, and thereby generating a more uniform slip ratio distribution within each axle. This also provokes more uniform slip angles between the front and rear axles, with a decrease of the overall lateral slip power loss. This benefit is relevant at high lateral accelerations, for which lateral tire slip is the most significant cause of power loss [1, 5, 8]. Although tire rolling resistance power losses are an important contribution, they do not change with the yaw moment generated by the torque-vectoring controller. As a consequence, they are not relevant to this analysis.

An extensive literature [6-8] discusses how EV energy efficiency can be improved by setting the most appropriate wheel torque distribution to achieve the reference traction force and yaw moment, the latter aiming at a target understeer characteristic. However, to the knowledge of the authors there is an important gap in assessing and predicting the impact of the reference level of EV understeer on energy efficiency. This contribution presents a set of experimental skidpad tests executed with a torque-vectoring-controlled EV, i.e., the prototype Range Rover Evoque of the European Union FP7 project iCOMPOSE, consisting of four on-board electric drivetrains. The analysis includes the evaluation of the power consumption corresponding to different reference understeer characteristics. The novel results permit an appreciation of the significance of the reference cornering response on the EV power input, and provide useful design guidelines.

2 Experiments

2.1 The vehicle demonstrator

The study was conducted on an electric Range Rover Evoque prototype with four identical on-board drivetrains, each of them consisting of a switched reluctance electric motor, a double-stage single-speed transmission system, constant velocity joints and a half-shaft. The vehicle demonstrator is shown in Figure 1.

The simplified schematic of the vehicle control system is reported in Figure 2. The control structure consists of three main layers:

i) A reference generator (Layer 1), responsible for defining the target values of the vehicle states (such as the reference yaw rate, r_{ref}) starting from the driver inputs (i.e., the steering wheel angle, δ, and the accelerator and brake pedal positions, p_a and p_b), and the measured or estimated vehicle states (e.g., vehicle speed, V, and longitudinal acceleration, a_X);

ii) A high-level controller (Layer 2), generating the overall traction/braking force and yaw moment demands, F_X^c and M_Z^c, to achieve the reference values of the vehicle states. M_Z^c is the yaw moment contribution caused by the torque-vectoring controller, i.e., by the difference among the wheel torques on the left- and right-hand sides of the vehicle (M_Z^c does not include the yaw moment contribution caused by the lateral tire forces);

iii) A low-level controller (i.e., the 'control allocator' in Figure 2, Layer 3), which outputs the reference torques, $\tau_{d,i}$, for the individual wheels (see the numbering conventions in the figure), corresponding to the values F_X^c and M_Z^c from the high-level controller in ii). $\boldsymbol{\Theta}$ is the vector of parameters (such as V) required for the calculation of the optimal wheel torque distribution (see [6]).

In particular, during the tests of this study the integral sliding mode controller described in [9] was adopted as yaw moment controller in Layer 2 (see Figure 2). Within Layer 3, the control allocator calculates the torque demand for the left and right sides of the vehicle, respectively $\tau_{d,L}$ and $\tau_{d,R}$, according to:

$$\tau_{d,L} = 0.5\left(F_X^c - \frac{M_Z^c}{d}\right)R$$
$$\tau_{d,R} = 0.5\left(F_X^c + \frac{M_Z^c}{d}\right)R \quad (1)$$

being d the half-track (assumed to be the same at the front and the rear axles), and R the wheel radius. During normal vehicle operation the torque demand for each side is efficiently split between the front and rear drivetrains according to the control allocation algorithm described in [6]. However, to avoid proliferation of results, during this study the torque demand was evenly distributed between the front and rear drivetrains on each side of the vehicle:

$$\tau_{d,1} = \tau_{d,3} = \frac{\tau_{d,L}}{2}$$
$$\tau_{d,2} = \tau_{d,4} = \frac{\tau_{d,R}}{2} \quad (2)$$

Eq. (2) simplifies the interpretation of the experimental results, which are affected only by the reference understeer characteristic.

Figure 1. The Range Rover Evoque vehicle demonstrator

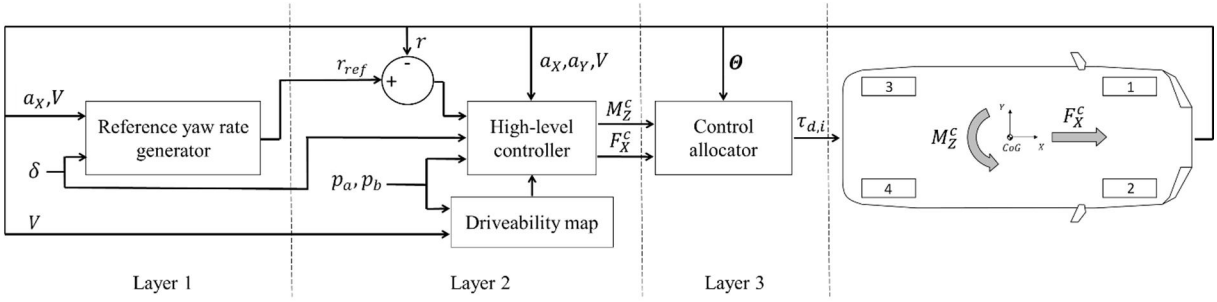

Figure 2. Simplified schematic of the vehicle control system

2.2 Understeer characteristics and test procedure

The derivation of the understeer characteristic providing maximum energy efficiency is based on experimental skidpad tests, in which the car negotiates a circular path with 60 m radius. The skidpad tests were executed at the Lommel proving ground (Belgium) for four different values of lateral acceleration (a_Y), i.e., ~2, 4, 6 and 8 m/s^2, corresponding to vehicle speeds of ~39, 56, 68 and 79 km/h. A Proportional Integral (PI) speed tracking controller guaranteed that the specified speed was maintained, so that the driver

had to control only the steering wheel, to keep the car on the circular trajectory. During the tests, the overall drivetrain power P was calculated as the battery power output:

$$P = V_{batt} I_{batt} \tag{3}$$

being V_{batt} and I_{batt} respectively the battery voltage and current. V_{batt} and I_{batt} were measured through a TA057 Pico Technology voltage sensor and an HTR400-SB LEM current sensor.

Figure 3 reports the experimentally measured points of the eleven understeer characteristics that were tested: the one of the passive vehicle (denoted as PV), five characteristics with progressively increasing understeer (denoted as U1, U2, …, U5), and five characteristics with progressively decreasing understeer (denoted as O1, O2, …, O5) with respect to the passive vehicle. The passive vehicle is understeering, i.e., the required steering input increases with lateral acceleration, as for any passenger vehicle.

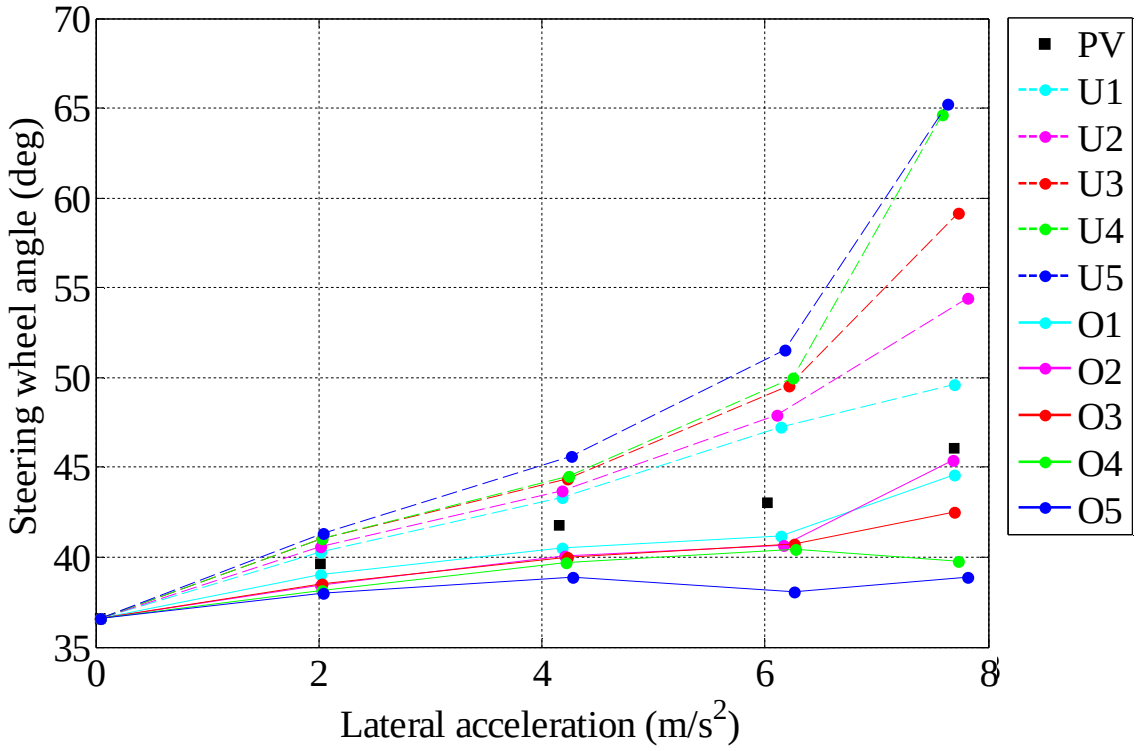

Figure 3. The experimentally measured understeer characteristics

For the tests an appropriate formulation of the reference yaw rate in Layer 1 was implemented to achieve the reference understeer characteristics. The tests were executed according to the following steps:

i) The battery was fully charged;
ii) The vehicle was accelerated from standstill to the specified speed on the circular trajectory through the PI speed tracking controller;
iii) When a steady-state condition was reached, trajectory and speed were maintained for two laps;
iv) Steps i)-iii) were repeated four times;
v) Steps i)-iv) were repeated for all the specified understeer characteristics and vehicle speeds.

3 Results

Figure 4 shows the average yaw moment demands, M_Z^c, generated by the yaw rate controller in Layer 2 as functions of lateral acceleration, which were used to track the reference yaw rate. Positive yaw moments

correspond to a destabilizing control action, i.e., less understeer, while negative yaw moments generate a stabilizing effect, i.e., they provoke increased understeer.

The average values of the measured drivetrain power input against a_Y are reported in Figure 5. In general, the power input varies in a repeatable and significant manner with changes of the reference yaw rate and understeer characteristic. However, from Figure 5 it is difficult to distinguish the trends corresponding to the different reference cornering responses, as the variation of power input is not a monotonic function of the level of vehicle understeer.

As a consequence, the power consumptions of the experimentally measured points were plotted as functions of steering wheel angle and lateral acceleration (see Figure 6). The experimental power input data were interpolated to obtain the power input map, $P(a_Y, \delta)$. The interpolated power profile was used to calculate the value of δ minimizing P for each assigned value of a_Y. In formulas:

$$\delta_{opt} = \arg min P(\delta)|_{a_Y=constant} \quad (4)$$

A selection of optimal steering angles, $\delta_{opt}(a_Y)$, is indicated in Figure 6 with the black solid circles. Figure 6 also reports the iso-curves for the relative drivetrain power input increase ($\Delta P\%$, expressed in percentage) with respect to the optimal understeer characteristic, $\delta_{opt}(a_Y)$ (see the contour curves at 5%, 9%, 13%, and 17%, and the respective color bar).

The black squares indicate the understeer characteristic of the passive vehicle. Interestingly, the optimal understeer characteristic always implies less understeer with respect to the passive vehicle, with an overall cornering behavior close to neutral steering (i.e., with an approximately constant steering wheel angle regardless of the lateral acceleration value). In comparison with the passive vehicle, the adoption of the optimal understeer characteristic allows energy savings of up to ~11%. For the case study vehicle these potential energy savings are even more significant than those achievable through the optimization of the control allocation algorithm (Layer 3 in Figure 2) [6].

For completeness, Figure 7 shows the $\Delta P\%$ contour plots on the graph of the reference yaw moment, M_Z^c, as a function of lateral acceleration, obtained with the same procedure as in Figure 6. The optimal yaw moment values, $M_{Z,opt}^c(a_Y)$, corresponding to $\delta_{opt}(a_Y)$, are indicated by the black solid circles. $M_{Z,opt}^c$ is monotonically increasing with a_Y. For a given a_Y, starting from the lower bounds of M_Z^c, $\Delta P\%(M_Z^c)$ is characterized by:

i) A reduction as a function of M_Z^c, for low (negative) values of M_Z^c. For example, for $M_Z^c < 0$, if a_Y~6 m/s^2, $\Delta P\%$ decreases from more than 9% (at the lower bound of the measured region) to less than 5%, where a local minimum is reached;

ii) A progressive increase, which brings a local maximum of $\Delta P\%$ for M_Z^c values close to zero;

iii) A progressive reduction for relatively small positive values of M_Z^c, until $\Delta P\%$ goes to zero, thus reaching its absolute minimum at $M_{Z,opt}^c$;

iv) An increase for significantly positive values of M_Z^c, with $\Delta P\%$ > 9% at the top boundary of the measured region. The nearly symmetric behavior of the $\Delta P\%$ contour characteristics (even if the absolute minimum, i.e., $\Delta P\%$ = 0, is always reached for $M_Z^c > 0$) with respect to the axis $M_Z^c = 0$ of Figure 7 will be the subject of further investigations.

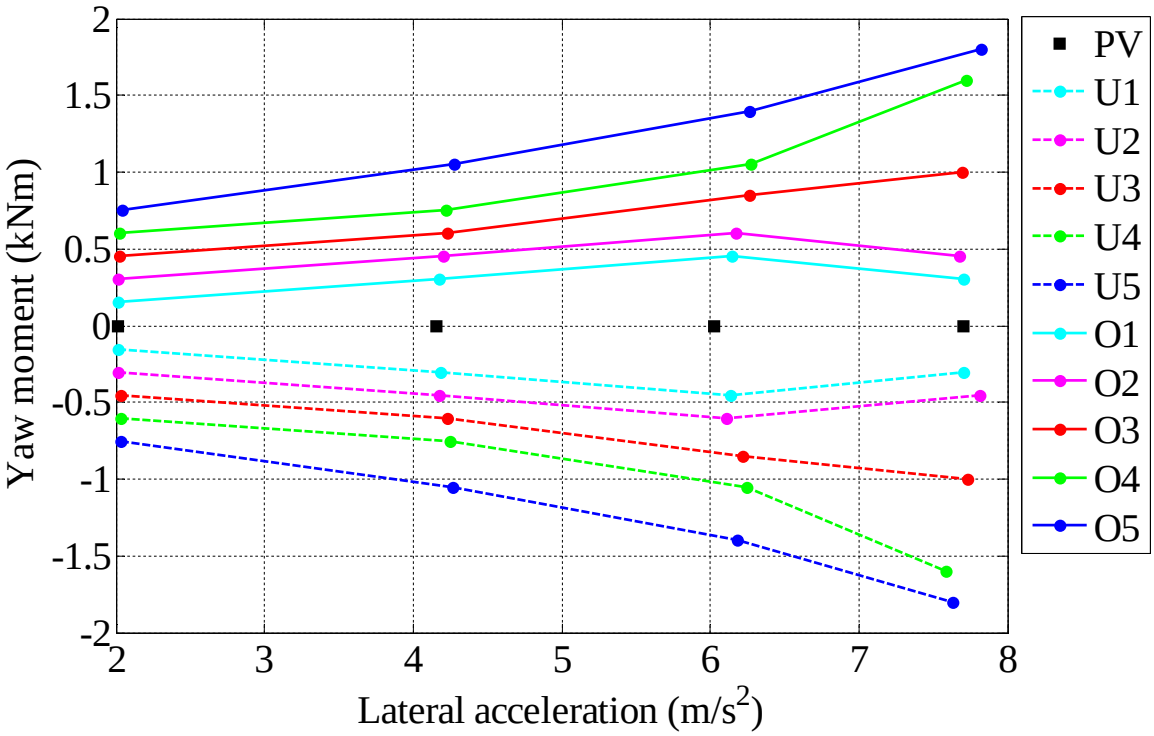

Figure 4. Reference yaw moment as a function of lateral acceleration, for different understeer characteristics

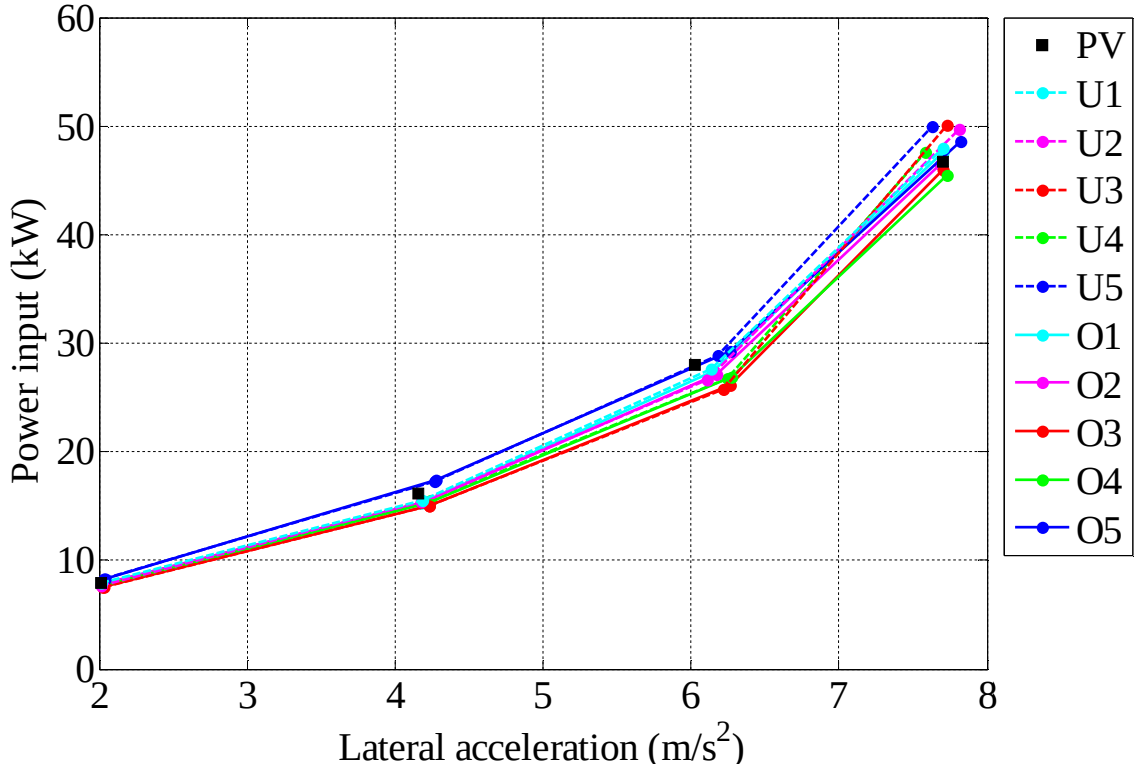

Figure 5. Power input as a function of lateral acceleration, for different understeer characteristics

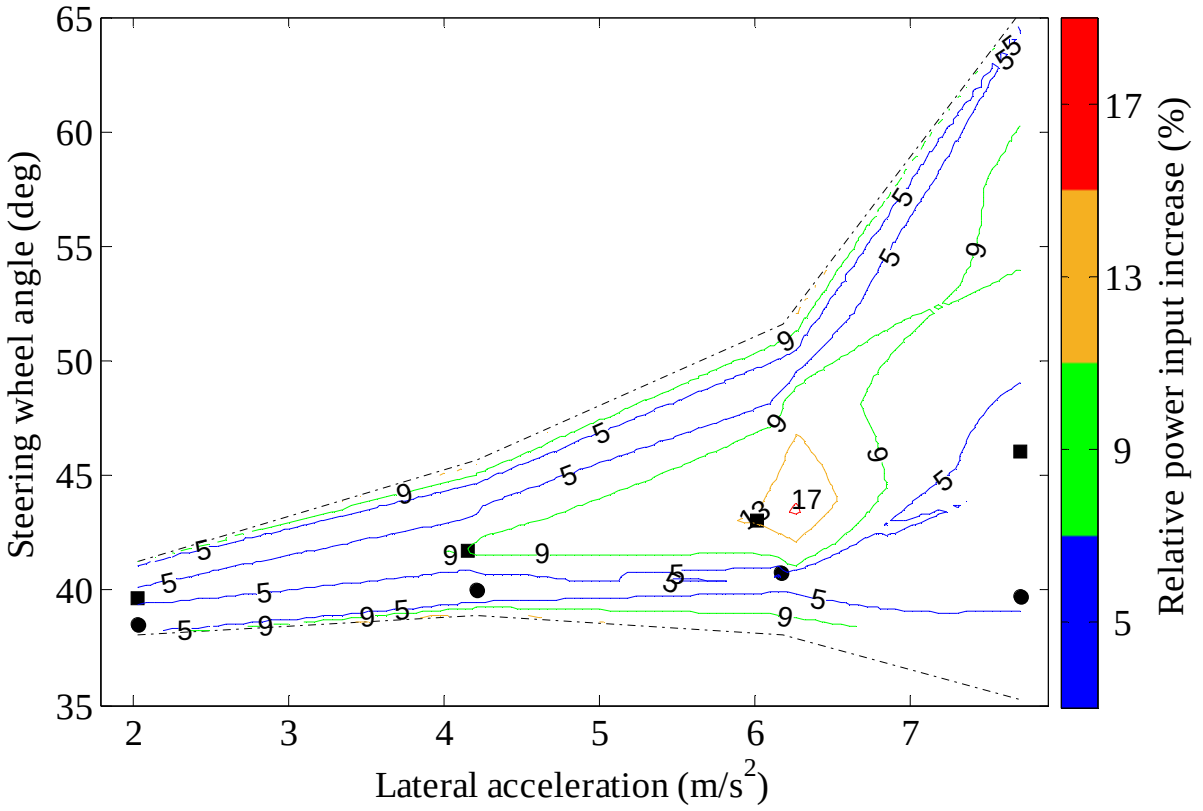

Figure 6. $\Delta P\%$ (contour plots); δ_{opt} (black solid circles); passive vehicle (black squares); boundaries of the measured region (dash-dotted lines)

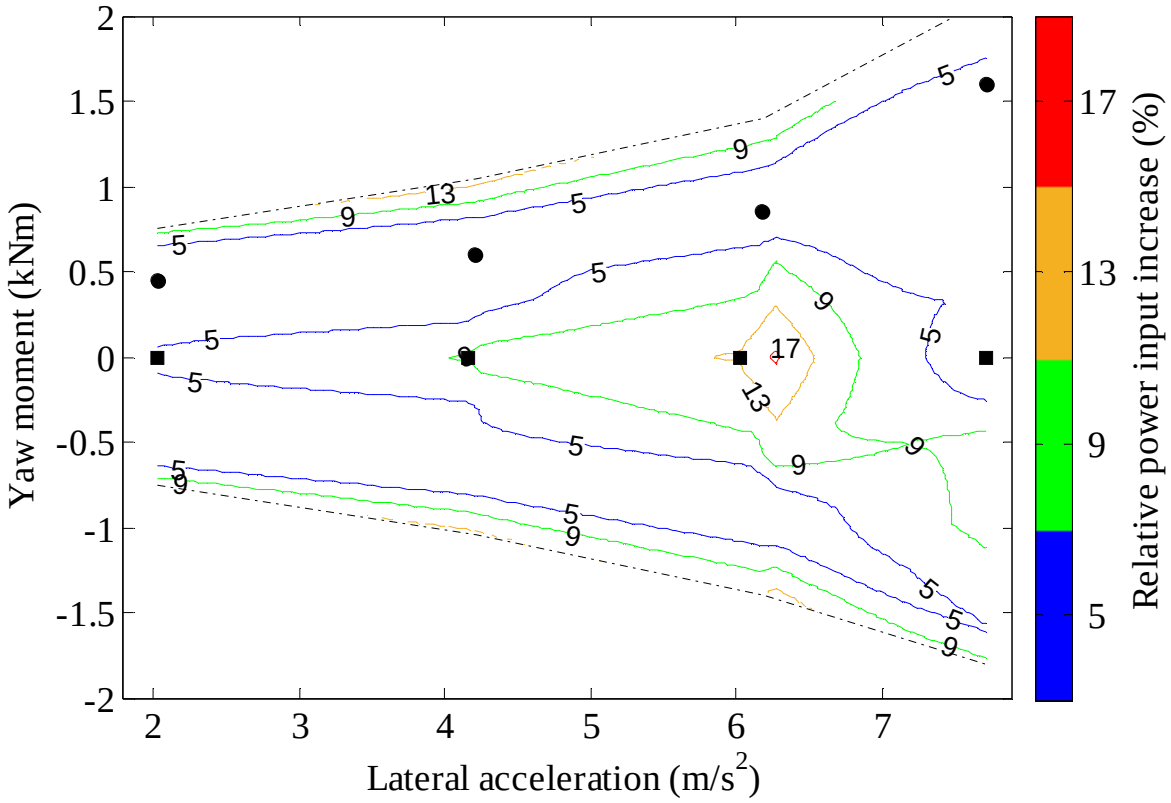

Figure 7. $\Delta P\%$ (contour plots); $M_{Z,opt}^{c}$ (black solid circles); passive vehicle (black squares); boundaries of the measured region (dash-dotted lines)

4 Conclusion

The presented experimental analysis allows the following conclusions:

- The variation of the reference yaw rate of the torque-vectoring controller has a significant impact on the energy consumption in cornering conditions;
- With a proper tuning of the reference cornering response, based on energy efficiency criteria and torque-vectoring, it is possible to obtain significant energy savings with respect to the passive vehicle. In particular, the optimal understeer characteristic brings measured input power reductions of up to ~11% for the case study vehicle demonstrator;
- The optimal understeer characteristic in terms of energy efficiency is close to the condition of neutral steering for the specific electric vehicle;
- For a given value of lateral acceleration, the pattern of the power loss variation as a function of the reference yaw moment is characterized by a relatively symmetric behavior, even if the absolute minimum is always achieved for destabilizing yaw moments.

Further work will propose a theoretical analysis supporting the experimental results, based on the investigation of the different power loss contributions, i.e., drivetrain and tire slip power losses. Moreover, energy-efficient wheel torque control allocation strategies will be implemented together with the optimal reference yaw rate characteristic obtained in this paper, to assess the overall power saving achievable with torque-vectoring control.

Acknowledgments

The research leading to these results has received funding from the European Union Seventh Framework Programme FP7/2007-2013 under grant agreement no. 608897.

References

[1] De Novellis, L., Sorniotti, A., Gruber, P. (2013). Optimal wheel torque distribution for a four-wheel-drive fully electric vehicle. SAE International Journal of Passenger Cars-Mechanical Systems, Vol. 6, Issue 1 (2013-01-0673), 128-136.

[2] Maeda, K., Fujimoto, H., Hori, Y. (2012). Four-wheel driving-force distribution method based on driving stiffness and slip ratio estimation for electric vehicle with in-wheel motors. Vehicle Power and Propulsion Conference, IEEE VPPC 2012.

[3] Feiqiang, L., Jun, W., Zhaodu, L. (2009). Motor torque based vehicle stability control for four-wheel-drive electric vehicle. Vehicle Power and Propulsion Conference, IEEE VPPC 2009.

[4] De Novellis, L., Sorniotti, A., Gruber, P. (2014). Design and comparison of the handling performance of different electric vehicle layouts. Proceedings of the Institution of Mechanical Engineers, Part D: Journal of Automobile Engineering, Vol. 228, Issue 2, 218-232.

[5] De Novellis, L., Sorniotti, A., Gruber, P. (2015). Driving modes for designing the cornering response of fully electric vehicles with multiple motors. Mechanical Systems and Signal Processing, Vol. 64-65, 1-15.

[6] Dizqah, A. M., Lenzo, B., Sorniotti, A., Gruber, P., Fallah, S., De Smet, J. (2016). A Fast and Parametric Torque Distribution Strategy for Four-Wheel-Drive Energy Efficient Electric Vehicles. IEEE Transactions on Industrial Electronics, in press.

[7] Yuan, X., Wang, J. (2012). Torque Distribution Strategy for a Front- and Rear-Wheel-Driven Electric Vehicle. IEEE Transactions on Vehicular Technology, Vol. 61, Issue 8, 3365-3374.

[8] De Novellis, L., Sorniotti, A., Gruber, P. (2014). Wheel Torque Distribution Criteria for Electric Vehicles with Torque-Vectoring Differentials. IEEE Transactions on Vehicular Technology, Vol. 63, Issue 4, 1593-1602.

[9] Goggia, T., Sorniotti, A., et al (2014). Integral Sliding Mode for the Torque-Vectoring Control of Fully Electric Vehicles: Theoretical Design and Experimental Assessment. IEEE Transactions on Vehicular Technology, Vol. 64, Issue 5, 1701-1715.

Authors

Basilio Lenzo received the MSc degree in mechanical engineering from University of Pisa and Scuola Superiore Sant'Anna, Pisa, Italy, in 2010, and the PhD degree in robotics from Scuola Superiore Sant'Anna, Pisa, Italy, in 2013. Since 2015, he has been a Research Fellow with the University of Surrey, Guildford, UK. His current research interests include vehicle dynamics, simulation and control.

Giovanni De Filippis received the MSc degree in mechanical engineering and the PhD degree in mechanical and management engineering from the Polytechnic University of Bari, Bari, Italy, in 2011 and 2015, respectively. Recently, he joined the University of Surrey, Guildford, UK, as Research Fellow in advanced vehicle engineering. His main research interests include structural identification and vehicle dynamics.

Aldo Sorniotti received the MSc degree in mechanical engineering and the PhD degree in applied mechanics from the Polytechnic University of Turin, Turin, Italy, in 2001 and 2005, respectively. He is a Reader of advanced vehicle engineering with the University of Surrey, Guildford, UK, where he is also the Coordinator of the Automotive Engineering Research Center. His main research interests include vehicle dynamics control and transmission systems for electric vehicles.

Patrick Gruber received the MSc degree in motorsport engineering and management from Cranfield University, Cranfield, UK, in 2005 and the PhD degree in mechanical engineering from the University of Surrey, Guildford, UK, in 2009. He is Senior Lecturer of advanced vehicle systems engineering with the University of Surrey. His current research interests include tire dynamics and development of novel tire models.

Koen Sannen received the MSc degree in motorsport engineering from Oxford Brookes University, Oxford, UK, in 2009. Since 2014, he has been a Researcher with Flanders MAKE, Lommel, Belgium. His main research interests include electro-mechanical systems in vehicles and machines.